Nigerian Journal of Technology (NIJOTECH)
Vol. 43, No. 1, March, 2024, pp.44 - 50
www.nijotech.com

Print ISSN: 0331-8443
Electronic ISSN: 2467-8821
https://doi.org/10.4314/njt.v43i1.6

NUMERICAL METHOD FOR PREDICTING FIRST CRACK LOAD ON HOLLOW-CORED BEAMS SUBJECTED TO POINT LOAD AT MIDSPAN

AUTHORS:
O. U. Orie[1], and U. K. Ogbonna[2,*]

AFFILIATIONS:
[1,2]Department of Civil Engineering, University of Benin, Edo State, Nigeria.

***CORRESPONDING AUTHOR:**
Email: engrogbonnaku@gmail.com

ARTICLE HISTORY:
Received: 02 November, 2023.
Revised: 14 January, 2024.
Accepted: 15 January, 2024.
Published: 31 March, 2024

KEYWORDS:
First crack load, Hollow cored beams, Modulus of Rupture, Moment of Inertia, Numerical method.

ARTICLE INCLUDES:
Peer review

DATA AVAILABILITY:
On request from author(s)

EDITORS:
Ozoemena Anthony Ani

FUNDING:
None

Abstract

Predicting the initial crack load in concrete is important to detect early warning of a problem. In this study, a model for predicting the first crack load on a hollow-cored rectangular beam point loaded at mid-span was developed by combining a numerical method and an experimental approach. The modulus of rupture was introduced into the governing moment-curvature relationship. Experimentally, flexural testing with point loads at mid-span was performed on fifteen (15) beams made up of three (3) beam types at 1 kN intervals for a span of 750mm using the Universal Testing machine. The beams were simply supported by roller points. The dimensions of the beams were kept constant and later varied while investigating the following hollow diameters: 0, 30, 60, 75, and 105mm. Numerically, the beams were designed as a beam element point loaded at mid-span with a span of 700mm centers, and the support conditions were defined as pinned support. Governing equations relating failure load with the modulus of rupture, stiffness matrix, shape functions, and moment of inertia were developed. The equation for predicting the first crack load, incorporating the modulus of rupture, was derived. The moment of inertia was calculated by discretizing the hollow-cored beam section using an isoparametric geometric transformation. The experimental results were used to validate the numerical model. 90.55% agreement between experimental and numerical results was observed. The overall average percentage difference between the two methods recorded is 9.45%. This shows that at about 91% confidence level, both approaches are the same and can be applied with confidence in the prediction of the first crack load on hollow-cored reinforced concrete beams.

1.0 INTRODUCTION

There are many existing structural members with hollow parts. It is evident that the addition of hollow cores to sections produces greater flexural strength and stiffness than solid components. In some circumstances, using hollow-reinforced horizontal members could be more cost-effective than using solid concrete members to reduce weight and cost [1]. Because concrete's tensile strength is so low, cracks in RC construction are unavoidable. When concrete experiences more tensile stress than it can withstand, cracks result. A crack in an RC member poses an ongoing threat to the structure's ability to operate as intended and to be serviceable; it has a big impact on serviceability, durability, aesthetics, and force transfer [2].

Numerous scholars have created advanced analytical techniques and made significant advances to our understanding of concrete behavior. Although these

HOW TO CITE:
Orie, O. U., and Ogbonna, U. K. "Numerical Method for Predicting First Crack Load on Hollow-Cored Beams subjected to Point Load at Midspan", *Nigerian Journal of Technology*, 2024; 43(1), pp. 44 – 50; *https://doi.org/10.4314/njt.v43i1.6*

accomplishments are widely documented and available in several reports and technical papers, there are still many areas that require a lot of understanding and research. A better understanding of the behavior of concrete has been made possible over the past ten years due to improvements in computing methods and the computational power of powerful computers. Finite element software can be used to analyze any structure as a whole or as a component of it, and the accuracy of the analysis is entirely dependent on the input values, particularly the material properties utilized. However, dealing with concrete requires a solid technical foundation to use it correctly and get the intended results [3].

2.0 LITERATURE REVIEW

The influence of altering the effective flange width and hollow core position in the compression zone of a plain concrete beam with a point load at mid-span was investigated to determine the ideal cored section of a hollow concrete beam. Equations were derived using the double integration method to determine the moment of inertia of the sections and corresponding deflections as the load increased until failure, while maintaining a constant cross-sectional area and randomly changing the section dimensions in 10mm increments from 150mm to 190mm flange width. The acquired results were compared to experimental results that had been linearized. The findings demonstrated that when the flange width increased, the beam samples' deflection with failure loads increased [4].

[5], conducted an experimental and numerical study on the effects of non-uniform reinforcement ratios along the length of reinforced concrete beams on their flexural behavior. The experiment used four reinforced concrete beams, each with a different reinforcement ratio. However, in the constant moment zone, three of the four beams' reinforcement ratios were similar. Cracking load and deflection were measured continuously during the test. Nonlinear finite element software was used to mimic the experimental behavior, which was then analyzed parametrically. The tension stiffening in reinforced concrete beams was found to be determined by the concrete area in the tension zone rather than the reinforcement ratio. Finite element analysis was used to accurately anticipate the behavior of reinforced concrete beams.

[6], examined the impact of distortional deformation on the elastic lateral buckling of thin-walled box beam elements under combined bending and axial stresses and established an analytical model for the stability of laterally unrestrained box beams by following higher-order theory. The governing equilibrium equations were discretized using Ritz and Galerkin's methods, and the buckling loads were then obtained by requiring the singularity of the tangential stiffness matrix. The various approaches were discussed, and then they were contrasted with the finite element simulation conducted using the Abaqus software using shell elements for the meshing process. The numerical results showed that, particularly for those thin-walled box beam members with high ratios between the height and thickness of the cross-section, conventional stability solutions like those used in Eurocode 3 overestimated the lateral buckling resistance.

An approach that could result in weight reduction and material savings is the partial replacement of the concrete beneath the neutral axis. [7] conducted an experimental and analytical investigation into the possibility of replacing some of the concrete in the tension zone below the neutral axis with air gaps. Polyethylene balls and PVC tubing were used to make air voids. PVC pipes and polyethylene balls in varying proportions were used to cast beams. Comparisons were made between the results for the control specimens, the polyethylene ball-and-pipe beams, and the PVC-pipe beams. Additionally, analytical analysis of the same was carried out using ANSYS to model the beam's flexural and shear behavior using the finite element method.

The shear stresses of a three-meter-long cantilever beam supplied with a point load at its free end were examined by [8]. Three cross sections were considered. In the study, maximum shear stresses produced using the following two techniques were compared using the finite element technique (FEM) and a traditional analytical equation. Both ANSYS and SAP2000 were used.

The results demonstrated a difference in the maximum shear stresses obtained by the software versus the analytical equation, with the latter usually being higher. Independent of the cross-section, the average deviations for ANSYS and SAP2000 were 12.76% and 11.96%, respectively. To generate more accurate findings, correction factors were introduced to the traditional analytical formula for each cross section situation. Analytically and numerically, the flexural properties of Hollow-Cored Reinforced Concrete Beams point loaded at mid-span were examined by [9]. Isoparametric geometric transformation of the coordinates was employed in discretizing the hollow-cored beam section numerically. Shape functions

were generated at each node using a 9-noded lagrangian quadratic element for the rectangular section and an 8-noded serendipity cubic element for the circular-hollow section. The moment of inertia was numerically calculated using double integration of the equations relating the shape functions and the Jacobian determinant for the reference coordinates.

Additionally, numerical solutions to the governing matrix equations connecting deflection and ultimate load were developed. It was observed that the analytical and numerical results were in agreement. The authors found that, when employing a finite element numerical technique, the diameter of hollow-cored beams increased both the moment of inertia and ultimate failure loads of the beams, while the deflection increased until the diameter reached 30 mm, after which the deflection decreased.

To close the gap in the reviewed literature, this study employs a computational method to forecast the first crack load of point-loaded rectangular hollow cored reinforced concrete beams at midspan, utilizing the modulus of rupture as the maximum stress criterion. The experimental results confirmed the validity of the numerical method.

3.0 MATERIALS AND METHODS

3.1 Materials

A recommended concrete mix proportion of cement, fine and coarse aggregates of 1:2:4 by weight with a water cement ratio of 0.5 in 28 days was used to produce the hollow cored beams. The mix proportion gave the characteristic strength f_{cu} of 20N/mm^2. The mix ratio was kept constant throughout the test with cubes made from each batching. The cubes were tested at 7, 14, and 28 days respectively. Crushed granite was used, the maximum size of which was 19mm. The coarse aggregate's grading and characteristics were per COREN Publication on Concrete mix design [10]. The fine aggregate was graded according to zone 3. Portland limestone cement (P.L.C) manufactured by Dangote cement company was used and designated as CEM II according to [11]. Mild steel (2R6) was provided in the tensile zone being the minimum reinforcement deduced. 2 legged 6mm diameter lateral ties @ 200 mm spacing were provided.

3.2 Methods

Flexural testing with point loads at mid-span was performed on the beams in the Laboratory. The load delivered by the universal testing machine was steadily increased until the first crack was observed. Readings were taken at 1kN intervals throughout the 750mm length. The beams are simply supported by roller points. Figure 1 shows the experimental setup. All details of the specimen's dimensions are illustrated in Table 1.

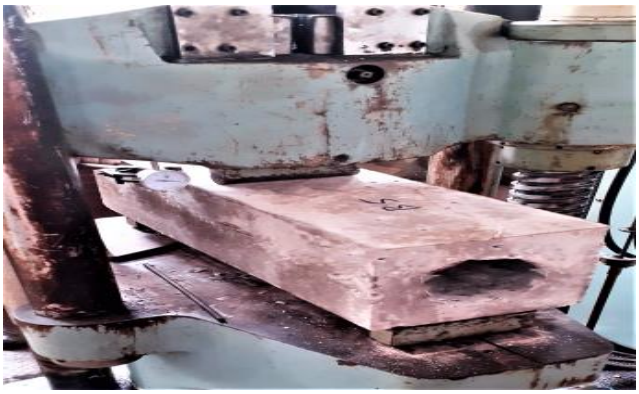

Figure 1: Experimental setup

3.2.1 Mixing, casting, and vibration

Due to the capacity of the concrete mixing equipment, batching was employed to mix the concrete. A weighed amount of cement and sand was poured into the mixer in the specified ratio, and mixing continued until an even mix was achieved. The specified weight of water was then added to the stated weight of coarse aggregate. The remainder of the specified water was added after a brief period of mixing, and the procedure was repeated until a homogenous concrete mix was obtained. Then, after being poured into the molds, the concrete was placed on the vibrating table for compaction. The top was leveled, given a smooth finish, and the discrepancy in the mold fill during molding was made up for by trowelling.

3.2.2 Curing

The specimens were de-molded and placed in curing tanks and were completely submerged in water after being cast for twenty-four (24) hours. On 7, 14, and 28 days, the cube specimens was tested, respectively. The beams were subjected to testing for twenty-eight days.

3.2.3 Specimen preparation and identity

Timber forms, each 750mm long, were used to produce the specimen. According to [12], the timber form work for the control beam was constructed to a standard size of 150mm x 150mm x 750mm. To create the three types of beam specimens that were under investigation, three different types of molds were created, as shown in Table 1. Before casting the concrete, holes were formed in the specimens by drilling precise holes at the mold's two longitudinal ends and inserting pipes of varying diameters. These pipes were removed after the concrete had time to harden, about an hour after casting.

3.2.4 Beam elastic modulus

The modulus of elasticity was calculated from [13];

$$E_{c,28} = K_o + (0.2 f_{cu,28}) \quad (1)$$

Where; $E_{c,28}$: the modulus of elasticity at 28 days; $f_{cu,28}$: the characteristic cube strength at 28 days (in N/mm^2); K_o: a constant closely related to the modulus of elasticity of the aggregate (taken as 20 kN/mm^2 for Normal-weight concrete).

Hence, for concrete strength of 20N/mm^2, at 28 days

$E_{c,28} = 20 + (0.2x20x10^{-3}$

$E = 20.004 N/mm^2$

3.2.5 Beam reinforcement

Mild steel (2R6) was provided in the tensile zone being the minimum reinforcement deduced from [14]:

$Effective\ cover\ = 25mm, \phi\ = 6mm$

$Effective\ depth\ = 150 - 6 + (^6/_2) = 116mm$

Moment capacity, $M_R = 0.87 f_y A_s (d - {}^s/_2)$ (2)

Where;

$$s = \frac{0.87 f_y A_s}{0.45 f_{cu} b} \quad (3)$$

From trial mix design $f_{cu} = 20N/mm^2; s\ =\ 7.3mm$

$M_R\ =\ 1.4KNm$

$X_U = \frac{(0.87x250x56.556)}{(0.36x20x150x116)} = 0.079$

$$X_{max} = \frac{(0.0035)}{\left[0.0035 + \frac{(0.87x250)}{(200x10^3)} + 0.002\right]} = 0.531$$

For an under-reinforced section, $X_u < X_{max}$

Therefore the section is under-reinforced;

$$A_s = \frac{M}{0.87 f_y Z} \quad (4)$$

$A_s = \frac{(1.4x10^6)}{0.87x250x0.95x116} = 56.6\, {}^{mm^2}/_m$

(Provide 3Y6 bars for bottom and 2Y6 top)

Nominal shear reinforcement will be provided in compliance with BS 8110: part 5, 1985;

$$\frac{A_{sv}}{bS_v} = \frac{(0.4)}{0.87 f_y} \quad (5)$$

$S_v = 205mm$. Hence provide 2-legged 6mm Φ lateral ties @ 200 mm spacing.

3.2.6 The modulus of rupture, f_r

Exception for the asymptotic case of an infinitely deep beam, the entire cross-section of a concrete beam does not remain elastic up to the maximum load. The concept of modulus of rupture, f_r , is based on the elastic beam theory and is defined as the maximum normal stress in the beam calculated from the maximum (ultimate) bending moment M_u. As a result, f_r simply indicates the nominal strength, $f_r = \sigma_N$, which is a parameter of the maximum load having the strength dimension. To increase the cross section's moment capacity, the cracking releases energy and redistributes stress [15].

3.2.7 The moment of inertia

The moment of inertia of the hollow-cored beam section was calculated numerically by the geometric transformation of the hollow-cored beam section and reported in detail in [9]. The moment of inertia is given as:

$$I = \frac{bh^3}{12} - \frac{\pi R^4}{3.9275} \quad (6)$$

Where; I: Moment of inertia in mm^4; b: beam width in mm; h: depth of beam in mm; R: Radius of the hole in mm.

3.2.8 Development of the first crack load equation

Numerically, the predicted failure load was obtained from the Numerical Relationship between the modulus of rupture and the Predicted Failure load P_f. A problem of a rectangular beam element that is simply supported at both ends under axial point load is presented.

The moment-curvature equation according to [16] is given by;

$$M = EI \frac{\partial^2 y}{\partial x^2} \quad (7)$$

Since, $y = [N]\{\delta\}_e = [N_1 N_2 N_3 N_4]\{\delta\}_e$ (8)

Differentiating equation (8) and substituting into equation (7) we get;

$$M = EI \left[\frac{\partial^2 N_1}{\partial x^2} \frac{\partial^2 N_2}{\partial x^2} \frac{\partial^2 N_3}{\partial x^2} \frac{\partial^2 N_4}{\partial x^2}\right]\{\delta\}_e \quad (9)$$

Also,

$$M = [D][B]\{\delta\}_e \quad (10)$$

Where $[D]\ =\ EI$ (11)

and $[B] = \left[\frac{\partial^2 N_1}{\partial x^2} \frac{\partial^2 N_2}{\partial x^2} \frac{\partial^2 N_3}{\partial x^2} \frac{\partial^2 N_4}{\partial x^2}\right]$ (12)

This is the stress resultant curvature matrix;

Since; $\varepsilon = \frac{2x}{l_e} - 1$ (13)

$$\frac{\partial N_i}{\partial x} = \frac{\partial N_i}{\partial x} \frac{\partial \varepsilon}{\partial x} = \frac{\partial N_i}{\partial x} \frac{2}{l_e} \quad (14)$$

Differentiating equation (14) and substituting into equation (12) we have that;

$$[B] = \frac{4}{l_e^2} \left[\frac{\partial^2 N_1}{\partial \varepsilon^2} \frac{\partial^2 N_2}{\partial \varepsilon^2} \frac{\partial^2 N_3}{\partial \varepsilon^2} \frac{\partial^2 N_4}{\partial \varepsilon^2}\right] \quad (15)$$

Further simplification leads to;

$$[B] = \frac{4}{l_e{}^2}[6\varepsilon - (1-3\varepsilon)l_e - 6\varepsilon(1+3\varepsilon)l_e] \quad (16)$$

Substituting equation (11) and (16) into equation (10) and solving gives;

$$[M] = \frac{EI}{l_e{}^2}[6\varepsilon - (1-3\varepsilon)l_e - 6\varepsilon(1+3\varepsilon)l_e]\{\delta_e\} \quad (17)$$

But from the strain-displacement matrix for the beam element we have that;

$$\{\sigma\} = [D][B]\{\delta\}_e \quad (18)$$

At $\{\sigma\} = \{f_r\}$

Stress resultant is the moment which is given by;

$$M = \frac{I}{y}f_r \quad (19)$$

Substituting equation (19) into (17) we get that;

$$\frac{I}{y}\{f_r\} = \frac{EI}{L^2}[6\varepsilon - (1-3\varepsilon)l_e - 6\varepsilon(1+3\varepsilon)l_e]\{\delta_e\} \quad (20)$$

But,

$$\{\delta_e\} = \frac{L^3}{EI}\{P_f\}\begin{bmatrix} 12 & 6L & -12 & 6L \\ 6L & 4L^2 & -6L & 2L^2 \\ -12 & -6L & 12 & -6L \\ 6L & 2L^2 & -6L & 4L^2 \end{bmatrix}^{-1} \quad (21)$$

Substituting equation (21) into equation (20) and applying boundary conditions, and further simplification it follows that;

$$\{P_f\} = \frac{3.5}{yl_e}\{f_r\}\left[\frac{bh^3}{12} - \frac{\pi R^4}{3.9275}\right] \quad (22)$$

$$D_{min} = \left(1.67bh^3 - \frac{yP_f l_e}{5.71f_r}\right)^{0.25} \quad (23)$$

Where; P_f: Numerical predicted failure load in KN; $\{f_r\}$: Modulus of rupture in N/mm^2; I: Moment of inertia in mm^4; y: depth of neutral axis from the topmost fiber in the tension zone in mm; D_{min}: Minimum diameter of the hole for any known first crack load in mm; b: width of the beam in mm; h: depth of the beam in mm; l_e: midspan length in mm; $\{f_r\} = 0.7\sqrt{f_{ck}}$ (Portland cement Association, 15th Edition).

4.0 RESULTS AND DISCUSSION

In this section, a numerical value of the first crack load equation obtained in Equation (22) and (23) are presented for a hollow cored beam section simply supported at both ends and point loaded at mid-span. A comparison was made between the two approaches (numerical and experimental) in predicting the first crack load on the hollow cored beams.

The results obtained from the study are presented in Table 2 to Table 8. $P_{cr,Exp.}$, $P_{cr,NUM}$, $r\%$, p_d and a_d are the experimental first crack load, numerical first crack load, incremental percentage of first crack load, margin of percentage error, and the average percentage difference between the experimental and numerical results respectively. The obtained numerical results were compared to the experimental ones (Exp. Results) as reported in Table 2. It was also observed from the experimental results shown in Table 6, that for the type 1 beam, there was a 1.67%, 3.75%, and 14.42% decrease in first crack load at 60mm, 75mm, and 105mm hole diameters respectively. For the type 2 beam there was a 6.67%, 21%, 36.08%, and 68.83% increase in first crack load to 30mm, 60mm, 75mm, and 105mm hole diameters respectively. Type 3 beam showed a 3.25%, 8.42%, 12.92%, and 19.58% increase in first crack load to 30mm, 60mm, 75mm, and 105mm hole diameter respectively.

Table 1: Beam specifications

D_m(mm)	Type 1 beams		Type 2 beams		Type 3 beams	
	Width,b (mm)	Depth,h (mm)	Width,b (mm)	Depth,h (mm)	Width,b (mm)	Depth,h (mm)
0	150	150	150	150	150	150
30	150	150	150	155	155	150
60	150	150	150	165	165	150
75	150	150	150	175	175	150
105	150	150	150	201	201	150

For the numerical results shown in Table 7, for the type 1 beam, there was a 1.57%, 3.78%, and 14.38% decrease in first crack load at 60mm, 75mm, and 105mm hole diameters respectively. For the type 2 beam there was a 6.91%, 19.82%, 32.72%, and 68.66% increase in first crack load to 30mm, 60mm, 75mm, and 105mm hole diameters respectively. Type 3 beam showed a 3.22%, 8.76%, 13.36%, and 19.82% increase in first crack load to 30mm, 60mm, 75mm, and 105mm hole diameter respectively.

Table 2: Experimental and numerical First crack load

D_m(mm)	First crack Load(kN)					
	Type 1 beams		Type 2 beams		Type 3 beams	
	$P_{cr,Exp.}$	$P_{cr,NUM}$	$P_{cr,Exp.}$	$P_{cr,NUM}$	$P_{cr,Exp.}$	$P_{cr,NUM}$
0	12.86	11.81	12.86	11.81	12.86	11.81
30	12.85	11.80	13.72	12.60	13.27	12.20
60	12.66	11.63	15.38	14.13	13.95	12.81
75	12.38	11.37	17.09	15.70	14.52	13.34
105	11.01	10.11	23.88	21.94	16.15	14.84

This is attributable to the moment of inertia, which is a measure of the beam's ability to resist bending or load of higher magnitude before failing. Inserting holes in the beams affected the moment of inertia. For a constant width and depth, increasing the hole diameter reduced the moment of inertia, while for constant width and increasing depth, and constant depth with varying width, the moment of inertia increased. For both experimental and numerical approaches, Type 2 beams performed better, leading to P_{cr} *and* D_{min} values in Table 8. The comparison shows that the present numerical approach predicts a slightly lower value of the first crack load than the

experimental approach, which is an advantage as slightly lower values make it safe for design purposes. Figure 2, Figure 3, and Figure 4 show the first crack initiation on the bottom fiber of the hollow-cored beams on a Type 1 beam, a Type 2 beam, and a Type 3 beam respectively.

In summary, the overall average percentage difference between the two results recorded is 9.45%. These differences being less than 10% are quite acceptable in statistical analysis [17]. This means that, at about 91% confidence level, both approaches are the same and can be applied with assurance. Thus, the present model has some level of safety and can be used with confidence in predicting the first crack load on hollow cored beams.

Table 3: Margin of Percentage error between the experimental and numerical results

D_m(mm)	Type1 beam	Type 2 Beam	Type 3 Beam
	p_d%	p_d%	p_d%
0	9.58	9.58	9.58
30	9.66	9.38	9.60
60	9.49	9.41	9.30
75	9.61	9.72	9.23
105	9.54	8.64	9.41
a_d(%)	9.58	9.35	9.42
Total a_d(%)		9.45	

Table 4: First crack load with corresponding minimum diameter of holes

Beam Section	Type 3 Beam	
	P_{cr}(kN)	D_{min}(mm)
150x150	10.8	30.0
155x150	11.2	30.3
165x150	11.9	30.8
175x150	12.7	31.2
201x150	14.5	32.3

Table 5: Percentage incremental change in width and depth of beams

D_m(mm)	Type 2 Beam	Type 3 Beam
	d_{inc}%, Num.	b_{inc}%, Num.
0	0	0
30	3.3	3.3
60	10.0	10.0
75	16.7	16.7
105	33.3	33.3

Table 6: Incremental percentage of first crack load with respect to the control beam (Experimental)

D_m(mm)	Type 1 beam	Type 2 Beam	Type 3 Beam
	$r_{1,exp.}$%,	$r_{2,exp.}$%	$r_{3,exp.}$%
0	0	0	0
30	-0.08	6.67	3.25
60	-1.67	21.00	8.42
75	-3.75	36.08	12.92
105	-14.42	68.83	19.58

Table 7: Incremental percentage of first crack load with respect to the control beam (Numerical)

D_m(mm)	Type 1 beam	Type 2 Beam	Type 3 Beam
	$r_{1,num}$%	$r_{2,num}$%	$r_{3,num}$%
0	0	0	0
30	-0.08	6.91	3.22
60	-1.57	19.82	8.76
75	-3.78	32.72	13.36
105	-14.38	68.66	19.82

Table 8: First crack load with corresponding minimum hole diameter

Beam Section	Type 2 Beam	
	P_{cr}(kN)	D_{min}(mm)
150x150	10.8	30.0
150x155	11.6	30.8
150x165	13.1	32.3
150x175	14.8	33.7
150x200	19.3	37.3

Figure 2: Picture showing first crack on the hollow cored beams that emanated due to the point load on a Type 1 Beam

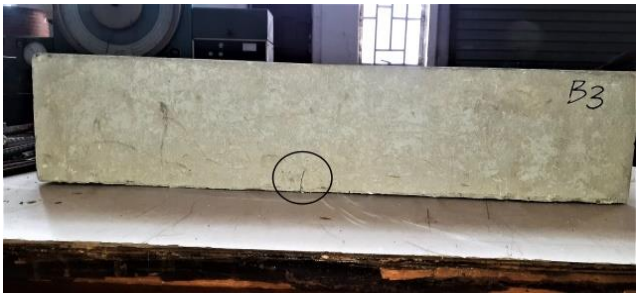

Figure 3: Picture showing first crack on the hollow cored beams that emanated due to the point load on a Type 2 Beam

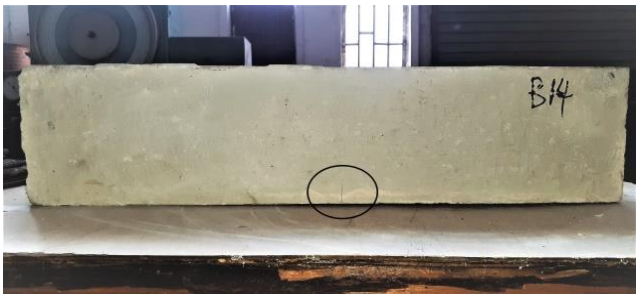

Figure 4: Picture showing first crack on the hollow cored beams that emanated due to the point load on a Type 3 Beam.

5.0 CONCLUSION AND RECOMMENDATION

This work set to develop and validate first crack equations for hollow cored beams. Numerical

solutions for predicting the first crack load have been developed by using numerical load deflection equation and incorporating the modulus of rupture as the failure criteria for first crack in concrete. The validation of the numerical method was carried out in an experimental setup. A good agreement between the Numerical and the experimental results were achieved in terms of first crack load for each hollow core diameter and beam cross section. From the result of this study as recorded in the percentage error analysis, it can be concluded that the numerical approach been an approximate relation for the experimental laboratory testing, provides a reliable solution in predicting first crack load and can be recommended for analysis of any type of rectangular hollow cored beam under simply support point load at mid-span.

REFERENCES

[1] Orie, O. E., and Idolor, B. "Optimizing Compression Zone Of Flanged Hollow Cored Concrete Beams Using Moment Of Inertia Theory", *Nigerian Journal of Technology (NIJOTECH)*. Vol. 34, Issue 2, pp. 217 – 222, 2015.

[2] Gund, A., and Pati, A. "Fracture Analysis Of Reinforced Concrete Beam", *International Research Journal of Engineering and Technology (IRJET)*, Volume: 07 Issue, pp. 186-190, 2020.

[3] Chaudhari, S. V., and Chakrabarti, M. A. "Modeling of concrete for nonlinear analysis Using Finite Element Code ABAQUS", *International Journal of Computer Applications*, Vol. 44, No.7, 2012, pp. 14-18.

[4] Orie, O. E., and Idolor, B. "Optimizing Compression Zone Of Flanged Hollow Cored Concrete Beams Using Moment Of Inertia Theory", *Nigerian Journal of Technology (NIJOTECH)*, Vol. 34, Issue 2, 2015, pp. 217 – 222.

[5] Daud, S. A., Daud, R. A., and Al-Azzawi, A. A. "Behavior of reinforced concrete solid and hollow beams that have additional reinforcement in the constant moment zone", *Ain Shams Engineering Journal*, Vol.12, Issue 1, 2021, pp 31-36.

[6] Saoul, A., Meftah, S. A., Mohri, F., and Daya, E. M. "Lateral buckling of box beam elements under combined axial and bending loads", *Journal of Constructional Steel Research*, Vol.116, pp. 2016,141-155.

[7] Soji, S., and Anima, P. "Experimental and Analytical Investigation on Partial Replacement of Concrete in the Tension Zone", *International Journal of Engineering Research and General Science*, Vol. 4, Issue 4, 2016,pp. 23-32.

[8] Al-Qasem, I., Hasan, A. R., Abdulwahid, M. Y., and Galobardes, I. "Comparison between Analytical Equation and Numerical Methods for Determining Shear Stress in a Cantilever Beam", *Civil Engineering Journal*, Vol. 4, Issue 2, 2018, pp.258-265.

[9] Orie, O. U., and Ogbonna, U. K. "Flexural Characteristics of Hollow Cored Rectangular plain Concrete Beams Using Finite Element Approach", *Journal of the Nigerian Association of Mathematical Physics*, Vol.62 Oct -Dec., 2021 Issue, 2021 pp147-152."

[10] Concrete Mix Design Manual First Edition: Council for the Regulation of Engineering in Nigeria, special Publication; No. Coren/2017/016/RC, August 2017.

[11] NIS444-1. Composition, Specification, and Conformity Criteria for Common Cements, Standard Organization of Nigeria, Lagos, 2014.

[12] British Standards Institution, BS 1881 part 109. "Specifications for Concrete Moulds", *British Standards House*, London, 1983.

[13] BS 8110 part 2-Code of Practice for special circumstances

[14] Mosley, W. H., and Bungey, J. H. Macmillan Education Ltd Reinforced Concrete Design, 1990.

[15] Novak, D., Bazant, Z. P., and Vitek, J. l. "Experimental - Analytical size - Dependent Prediction of Modulus Of Rupture of concrete", *Non-traditional cement and concrete*, 2002, pp.387-393.

[16] Bharikatti, S. S. "Finite Element analysis", 1st edition, *New age international (P) ltd*., New Delhi, India, 2005.

[17] Onyeka, F. C., Okeke, E. T., and Wasiu, J. "Strain–Displacement Expressions and their Effect on the Deflection and Strength of Plate", *Advances in Science, Technology and Engineering Systems*, 5(5), 2020, pp 401-413.